

The Mars orbiter magnetometer of Tianwen-1: in-flight performance and first science results

YuMing Wang^{1,2*}, TieLong Zhang^{2,3}, GuoQiang Wang⁴, SuDong Xiao⁴, ZhuXuan Zou^{1,2}, Long Cheng^{1,2}, ZongHao Pan^{1,2}, Kai Liu^{1,2}, XinJun Hao^{1,2}, YiRen Li^{1,2}, ManMing Chen^{1,2}, ZhouBin Zhang⁵, Wei Yan⁵, ZhenPeng Su^{1,2}, ZhiYong Wu^{1,2}, ChengLong Shen^{1,2}, YuTian Chi⁶, MengJiao Xu⁶, JingNan Guo^{1,2}, and Yang Du⁷

¹School of Earth and Space Sciences/Deep Space Exploration Laboratory, University of Science and Technology of China, Hefei 230026, China;

²CAS Center for Excellence in Comparative Planetology/CAS Key Laboratory of Geospace Environment/Mengcheng National Geophysical Observatory, University of Science and Technology of China, Hefei 230026, China;

³Space Research Institute, Austrian Academy of Sciences, Graz, Austria;

⁴Institute of Space Science and Applied Technology, Harbin Institute of Technology, Shenzhen 518055, China;

⁵National Astronomical Observatories, Chinese Academy of Sciences, Beijing 100012, China;

⁶Institute of Deep Space Sciences, Deep Space Exploration Laboratory, Hefei 230026, China;

⁷Shanghai Institute of Satellite Engineering, Shanghai 201109, China

Key Points:

- Magnetometer onboard Tianwen-1 orbiter performs well.
- 158 bow shock crossings are identified and statistically studied.
- The flank of Martian bow shock is more dynamic than its nose.

Citation: Wang, Y. M., Zhang, T. L., Wang, G. Q., Xiao, S. D., Zou, Z. X., Cheng, L., Pan, Z. H., Liu, K., Hao, X. J., ... Du, Y. (2023). The Mars orbiter magnetometer of Tianwen-1: in-flight performance and first science results. *Earth Planet. Phys.*, 7(2), 1–13. <http://doi.org/10.26464/epp2023028>

Abstract: The Mars Orbiter MAGnetometer (MOMAG) is a scientific instrument onboard the orbiter of China's first mission for Mars — Tianwen-1. Since November 13, 2021, it has been recording magnetic field data from the solar wind to the magnetic pile-up region surrounding Mars. Here we present its in-flight performance and first science results, based on its first one and one-half months' data. Comparing these early MOMAG observations to the magnetic field data in the solar wind from NASA's Mars Atmosphere and Volatile Evolution (MAVEN) mission, we report that the MOMAG magnetic field data are at the same level in magnitude, and describe the same magnetic structures with similar variations in three components. We recognize 158 clear bow shock (BS) crossings in these MOMAG data; their locations match well statistically with the modeled average BS. We also identify and compare five pairs of datasets collected when Tianwen-1's orbiter and the MAVEN probe made simultaneous BS crossings. These BS crossings confirm the global shape of modeled BS, as well as the south-north asymmetry of the Martian BS. Two cases presented in this paper suggest that the BS is probably more dynamic at flank than near the nose. So far, MOMAG performs well, and provides accurate magnetic field vectors. MOMAG is continuously scanning the magnetic field surrounding Mars. Data from MOMAG's measurements complement data from MAVEN and will undoubtedly advance our understanding of the plasma environment of Mars.

Keywords: Mars; magnetic field; Tianwen-1 magnetometer; bow shock

1. Introduction

Tianwen-1 is the first mission of China to explore and study Mars from its space environment to the surface (Wan WX et al., 2020; Zou YL et al., 2021). It consists of an orbiter, a lander, and a rover called Zhurong. The Mars Orbiter MAGnetometer (MOMAG) is one of the scientific instruments onboard the orbiter (Liu K et al., 2020). It investigates the magnetic field environment of Mars by measur-

ing the local vector magnetic field, and therefore provides key information for the understanding of the history and evolution of Mars.

The magnetic field surrounding Mars has two sources. One is the dynamic magnetic field resulting from the coupling between the solar wind and the Martian ionosphere; the other is the static crustal magnetic field of Mars itself. Since Mars has no global intrinsic magnetic field, the solar wind carrying the interplanetary magnetic field interacts directly with the Martian ionosphere, forming the "bow shock" (BS) and induced magnetosphere, which consists of the magnetic pileup region (MPR) and the wake region

Correspondence to: Y. M. Wang, ymwang@ustc.edu.cn

Received 29 NOV 2022; Accepted 13 JAN 2023.

Accepted article online 16 FEB 2023.

©2023 by Earth and Planetary Physics.

(e.g., Bertucci et al., 2004; Brain et al., 2006). Between the BS and the MPR, there is a magnetosheath separated from the MPR by the magnetic pileup boundary (MPB) (e.g., Mazelle et al., 2004). The magnetic field in these regions influenced by solar wind is highly dynamic.

Escape of ions in the Martian atmosphere is one of the core science issues to be addressed by Tianwen-1, and is closely related to the planet's magnetic environment. For example, the southern hemisphere's strong static crustal magnetic field may reach up to a high altitude and reconnect with the interplanetary magnetic field, causing the escape of ions (Brain et al., 2015), just like the behavior of Venus (Zhang TL et al., 2012). Besides, various waves in the ionosphere may heat particles, causing ion outflow (Ergun et al., 2006), and when these heated ions transport beyond the MPB, they will interact with the magnetic field carried by the solar wind stream to further generate ion cyclotron waves, boosting the escape of the ions (Russell and Blanco-Cano, 2007). The escape rate during storm times will be one to two orders higher than during quiet times (Jakosky et al., 2015b).

During November and December, 2021, the Tianwen-1 orbiter was running on a highly inclined and highly eccentric orbit (periapsis of about $1.08 R_M$, apoapsis of about $4.17 R_M$, as shown in Figure 1). During that period, the periapsis was right above the northern pole of Mars, the apoapsis far above the southern pole in the solar wind, and the orbital period was about 7.8 h, with about 50%–75% of its time in the solar wind. Thus, MOMAG mainly measured the magnetic field from solar wind to the MPR on the dawn-dusk side. Later, the inclination angle of the orbit will decrease, allowing the orbiter to detect the wake region of Mars. These data will help us understand the structure and evolution of the Martian magnetic field environment and provide clues for ion escape. Since the Mars Atmosphere and Volatile Evolution mission (MAVEN, Jakosky et al., 2015a), which also carries a magnetometer (MAG, Connerney et al., 2015), is still working, the successful operation of MOMAG will for the first time allow study of the Martian magnetic field environment from two observational points.

In this paper, we present and analyze data collected from November 15–December 31, 2021. In Section 2, we describe basic infor-

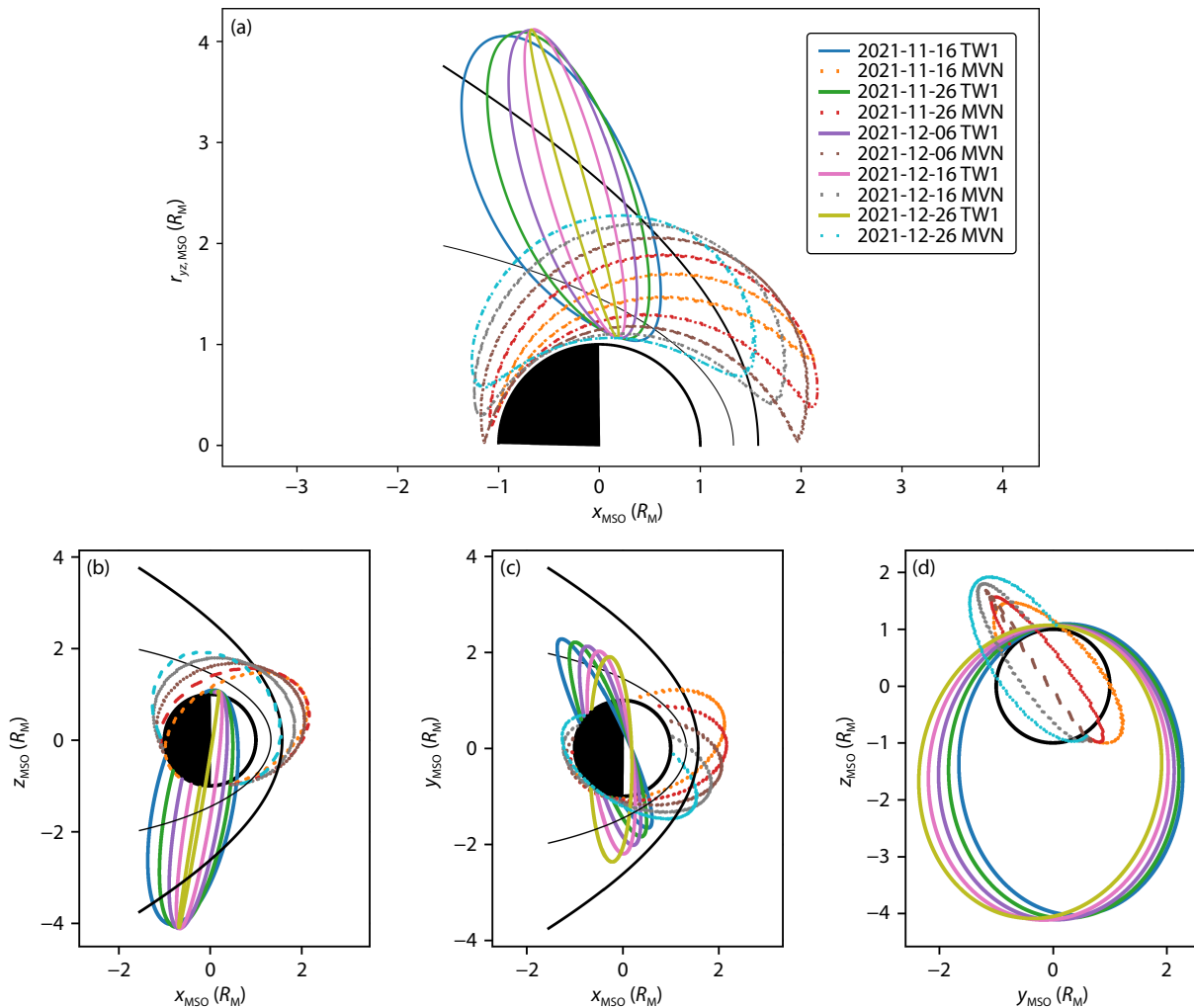


Figure 1. The orbits of Tianwen-1's orbiter (solid lines) and MAVEN (dashed lines) during November 13–December 31, 2021. The modeled Martian bow shock and MPB (Edberg et al., 2008) are indicated by thick and thin black lines, respectively. The different panels show the orbit from different angle of view as indicated by the horizontal and vertical axes.

mation about MOMAG and its current status, and present some of its magnetic field data. Then in Section 3 we show the first results of MOMAG regarding the Martian BS and compare them to MAVEN/MAG data. In the last section, we summarize the paper.

2. In-flight Calibration and Performance

The MOMAG contains two sensors mounted on a boom 3.19 m long. The outer sensor is at the top of the boom; the inner sensor is 0.9 m away (see Liu K et al., 2020 for details). Since the orbiter of Tianwen-1 does not have magnetic cleanliness control, the boom is actually not long enough to avoid contamination of the magnetic field from the structure of the orbiter. Thus, how to remove this interference from the magnetic fields measured by the two separated sensors becomes pivotal.

The procedure for mitigating the orbiter's distortion of the ambient magnetic field generally includes two steps, similar to the procedure applied to data from the magnetometer of the Venus Express (Zhang TL et al., 2008; Pope et al., 2011). The first step is to remove the magnetic interference due to the operations of the instruments. Such interferences behave as jumps in the magnetic field. If a real discontinuity in the solar wind passes the spacecraft, the amplitudes of the jump at the two sensors should be the same. However, since the two sensors are at different distances from the instrument, an artificial jump will show different amplitudes at the two sensors, and therefore can be distinguished from real jumps. For these artificial jumps, we remove them by the method of Pope et al. (2011). The second step is to remove the static magnetic field of the orbiter and correct the offset of the fluxgate magnetometer. This step is based mainly on the property of Alfvénic waves — that the magnetic field rotates almost in a plane without change of magnitude (Wang GQ and Pan ZH, 2021). We process the MOMAG raw data through these steps to scientific use level 2 (level C in China's convention). We iterate the procedure and reach the first version of the level 2 data, which can be found at the Planet Exploration Program Scientific Data Release System (<http://202.106.152.98:8081/marsdata/>). The data used in this paper and in our forthcoming papers will also be put on the official website of the MOMAG team at the University of Science and Technology of China (USTC, http://space.ustc.edu.cn/dreams/tw1_momag/). A complete description of the in-flight calibration procedure as well as a demonstration of the reliability of the calibrated data is given in the separate paper by Zou ZX et al. (2023).

Figure 2a shows the magnetic field in the Mars-centered Solar Orbital (MSO) system measured by MOMAG during 01:00–09:00 UT on 2021 December 30. The orbiter was unning in the magnetosheath before 02:55 UT; at around 03:01:25 UT the orbiter crossed the BS, where the amplitude of the magnetic field discontinuity was more than 10 nT (Figure 2h). After about four hours the orbiter again crossed the BS, where this time the amplitude of the magnetic field discontinuity was about 16 nT (Figure 2i). Around 08:20 UT, the orbiter even crossed the MPB. The BS during the second crossing was obviously stronger than that during the first crossing. The reason is that the BS was compressed during the second crossing, which can be seen from Figure 2d–g: the two BS crossings were on the south, the first crossing outside and further away from the modeled averaged BS (Edberg et al., 2008)

than the second BS crossing.

If we look into the details of the first BS crossing as shown in Figure 2h, it can be seen that the orbiter crossed beyond the BS at around 02:56:30 UT and crossed back in again at 02:57:30 UT before finally entering the solar wind. The magnetic field changes during these preceding crossings suggest that the BS was slightly stronger than the BS at 03:01:25 UT. This could also be explained as the compression of the BS. During these crossings, the orbiter was moving away from Mars as indicated by the color-coded orbit in Figure 2d. The locations of the preceding crossings were closer to Mars than that of the final crossing at 03:01:25 UT.

The magnetic fields in the solar wind stayed at around 9–10 nT, and fluctuated much less than those in the magnetosheath. Figure 2b displays the power spectral density of the magnetic field, generated by using a 10-min window and 1-min running step. It can be seen that the solar wind was indeed quiet except at very low frequency, whereas in the magnetosheath the magnetic fluctuation was enhanced. Behind the bow shock appear weak magnetic waves right below the proton gyro-frequency. In the solar wind, a small structure can be found between 05:15 and 06:35 UT. Though the total magnetic field is only slightly enhanced, the most notable change occurred for B_y , which decreased twice from about 4 nT to zero.

For comparison, Figure 3 shows the MAVEN measurements of the magnetic field and solar wind during 04:00–07:00 UT on the same day. MAVEN had a quite different orbit, its orbital period shorter than 4 hours (Figure 3c–g). Within one hour, it crossed the BS twice, but the positions of its crossings were both closer to the shock nose than those of Tianwen-1. Since the two crossings stay close to the same modeled BS, suggesting the solar wind conditions during the two crossings were almost the same, the amplitudes of their magnetic field discontinuities were similar. We show the detailed BS crossings in Figures 3h and i. No multiple BS crossings happened at MAVEN, probably suggesting different behavior of the BS at different locations.

Though the solar wind region that MAVEN detected was far away from that detected by Tianwen-1, a similar structure could be found between 05:20 and 05:55 UT (Figure 3a), which corresponds to the first dip recorded in MOMAG. During that time, the solar wind speed was about 310 km·s⁻¹ and the number density of protons was about 7 cm⁻³ (see the blue and red lines in Figure 3c). Different from MOMAG data, the magnetic field at MAVEN fluctuated considerably, notably at the proton gyro frequency (Figure 3b). This might be because MAVEN was closer to Mars than Tianwen-1 when they flew in the solar wind; particles escaping at a closer distance from the Martian atmosphere might more easily interact with the solar wind and interplanetary magnetic field to generate such fluctuations. However, according to the statistical study of MAVEN data (Ruhunusiri et al., 2017), such a pattern seems not to be evident and needs further validation.

3. Bow Shock Crossings

Bow shock is one of the notable features in the Martian space environment. Its shape may reflect upstream solar wind conditions

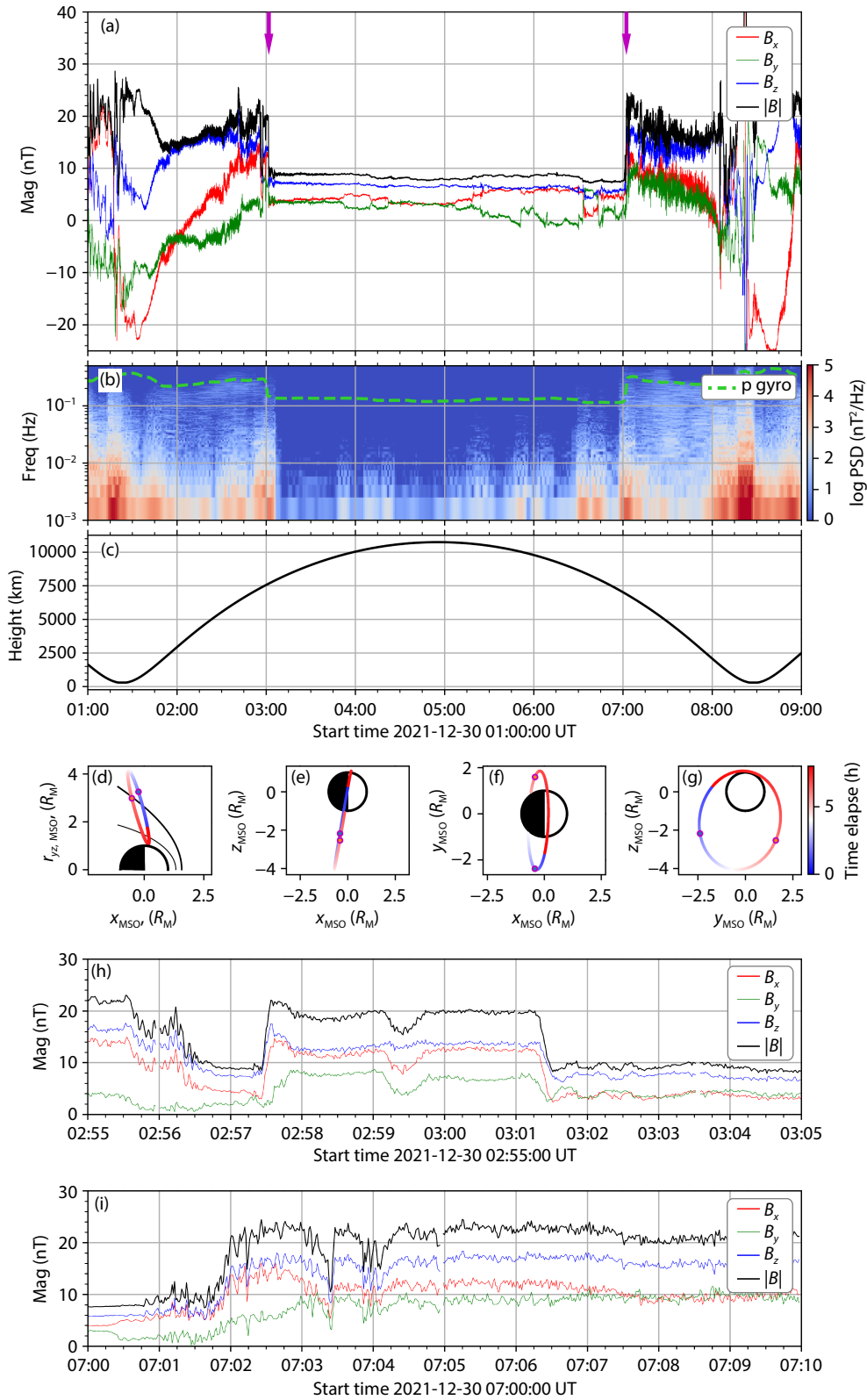


Figure 2. The magnetic field measured by MOMAG during 01:00–09:00 UT on December 30, 2021. Panel (a) shows the three components of the magnetic field in MSO coordinates with the total magnitude overplotted. Two purple arrows mark the crossings of the bow shock. Panel (b) shows the power spectral density of the magnetic field fluctuations. The green line indicates the proton’s gyro frequency. Panel (c) shows the height of the Tianwen-1 orbiter, and Panels (d)–(g) display its orbit in the MSO coordinates during the period of interest, in which the two circled dots mark the positions of the bow shock crossings. Note that Panel (d) is in the aberrated MSO coordinates with the modeled BS and MPB indicated by black lines. Panels (h) and (i) show the two BS crossings, respectively, in detail.

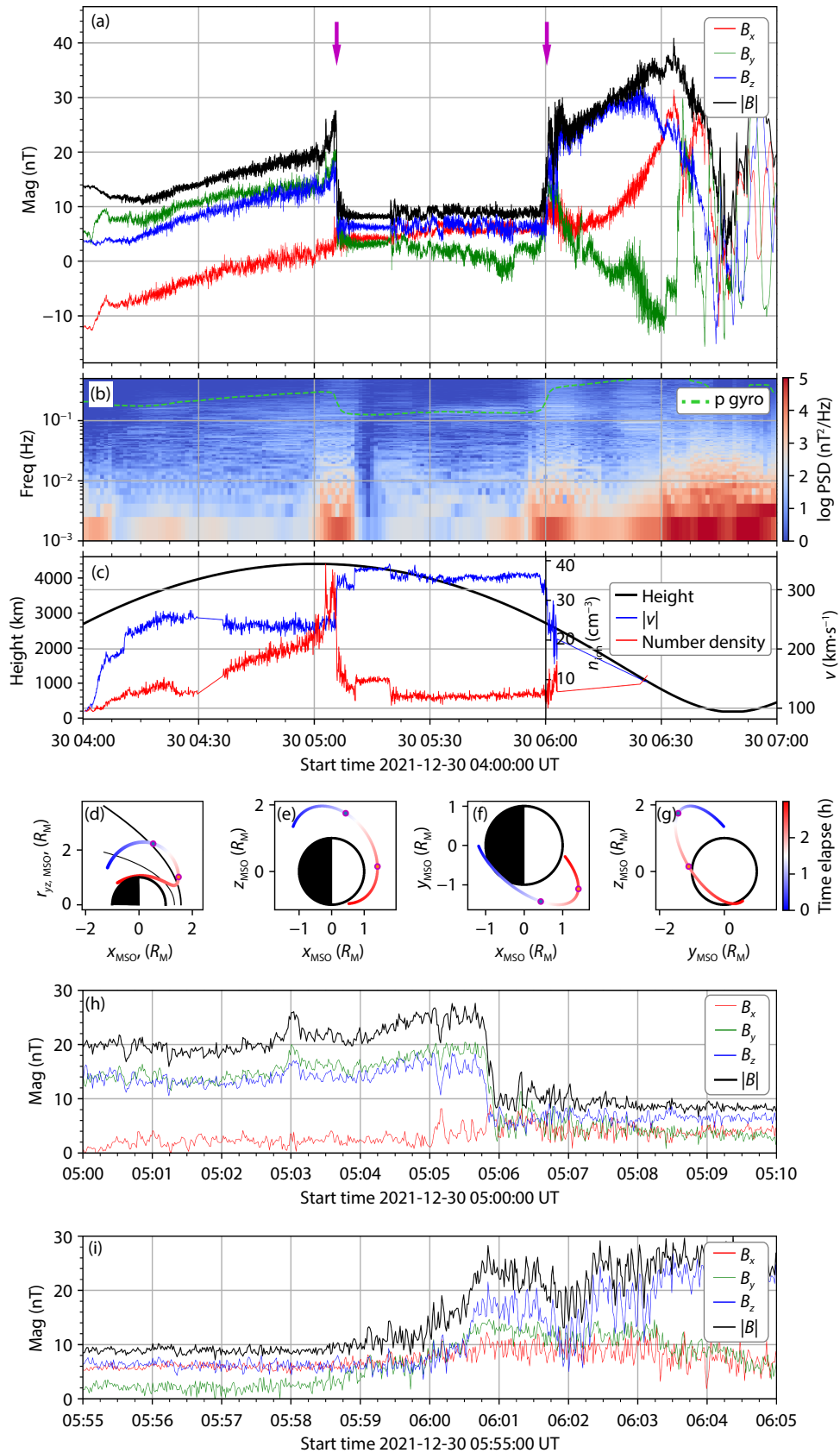


Figure 3. The magnetic field and solar wind plasma measured by MAVEN during the same period as Figure 2. In Panel (c) the solar wind speed and number density of ions are presented with the blue and red lines, respectively. The arrangements of other panels are the same as those in Figure 2.

and solar EUV intensity, and interaction processes between the solar wind and the Martian atmosphere (Mazelle et al., 2004; Ramstad et al., 2017; Hall et al., 2019). Thus, studying the Martian BS is our first choice to showcase the scientific potential of MOMAG data. In those data, collected from November 15–December 31, 2021, we recognize 158 BS crossings by manually checking the magnetic field strength variation and the fluctuation level (which is measured by the standard deviation of the magnetic field within each one minute interval). In principle, there should be more crossings, but Tianwen-1 crossed mostly the flank of the BS where the characteristic of a shock may be too weak to be recognized. In MAVEN/MAG data collected during the same period, we recognize 454 BS crossings.

Figure 4a shows all of the BS crossings in aberrated MSO coordinates (MSO coordinates are rotated by 4° about the z -axis to reduce the effect of the Mars orbital motion on the solar wind flow direction). Since the spatial coverage of the crossings is not wide enough to produce a plausible best-fit BS model, instead we compare these crossings data with the previously established BS model (Edberg et al., 2008). The data points in Figure 4a suggest that the crossings statistically match the model fairly well.

Martian BS position and global shape were derived from many single crossings. Now we can check this previous work, based on joint magnetic field observations from Tianwen-1/MOMAG and MAVEN/MAG. By assuming that the BS remains unchanged within 2 minutes, we use five instances of BS crossings of Tianwen-1 and MAVEN that occurred within 2 minutes of each other to examine the BS global shape. We choose 2 minutes because the upstream solar wind conditions that determine the BS position and shape, i.e., the fast-mode Mach number and dynamic pressure, are usually stable within this time-scale as revealed by the following analysis.

Figure 5a shows the characteristic speeds in the solar wind, calculated for every minute from November 15 to December 31, 2021, from MAVEN/SWIA (Halekas et al., 2017) measurements of the

solar wind velocity, ion density, and temperature and MAVEN/MAG measurements of the magnetic field. The Alfvén speed, v_A , ranges from almost zero to more than $100 \text{ km}\cdot\text{s}^{-1}$ with mode at around $30 \text{ km}\cdot\text{s}^{-1}$. Since Alfvén waves propagate along the magnetic field, if we take into account the direction of magnetic field, which mostly concentrates around 86° with respect to the x -axis in MSO (as indicated by the black line in Figure 5a), the Alfvén speed along the x -axis approaches zero. The sound speed, v_{cs} , is overall larger than the Alfvén speed, and is rarely smaller than $30 \text{ km}\cdot\text{s}^{-1}$. The fast-mode magnetoacoustic speed along the x -axis, $v_{f,x}$, with mode of roughly $60 \text{ km}\cdot\text{s}^{-1}$, is overall larger than both the Alfvén speed and the sound speed.

Since the solar wind propagates along the x -axis, and $v_{f,x}$ is the fastest among these characteristic speeds, the fast-mode Mach number in x -axis, $M_{f,x}$ is calculated. The black line in Figure 5b shows the median value of $M_{f,x}$ within one-minute intervals during the period of interest. We can read from the line that the dynamic range of $M_{f,x}$ is about 7, i.e., from about 2 to 9 with mode at about 6.2. We further examine the inhomogeneity of $M_{f,x}$ by calculating the difference between the maximum and minimum values of $M_{f,x}$ at various time scales, varying from one minute to 29 minutes as shown by the color-coded thin lines in Figure 5b. Each line presents the distribution of the difference (or range) of the $M_{f,x}$ in the given time scale. We can see that these distributions extend toward large values with increasing time scales, suggesting the enhancement of the inhomogeneity in terms of $M_{f,x}$. Then we determine the middle value of $M_{f,x}$ for each distribution, the value at which the distribution is divided equally, and define the inhomogeneity as the ratio of the middle value to the dynamic range of $M_{f,x}$. The dependence of the inhomogeneity on the time scale is plotted in Figure 5c. If we assume that an inhomogeneity of 0.1 is an acceptable level for a stale solar wind, we may conclude that the time scale of stable solar wind, in terms of $M_{f,x}$ is about 2 minutes.

A similar analysis is applied to the solar wind dynamic pressure, p_d ,

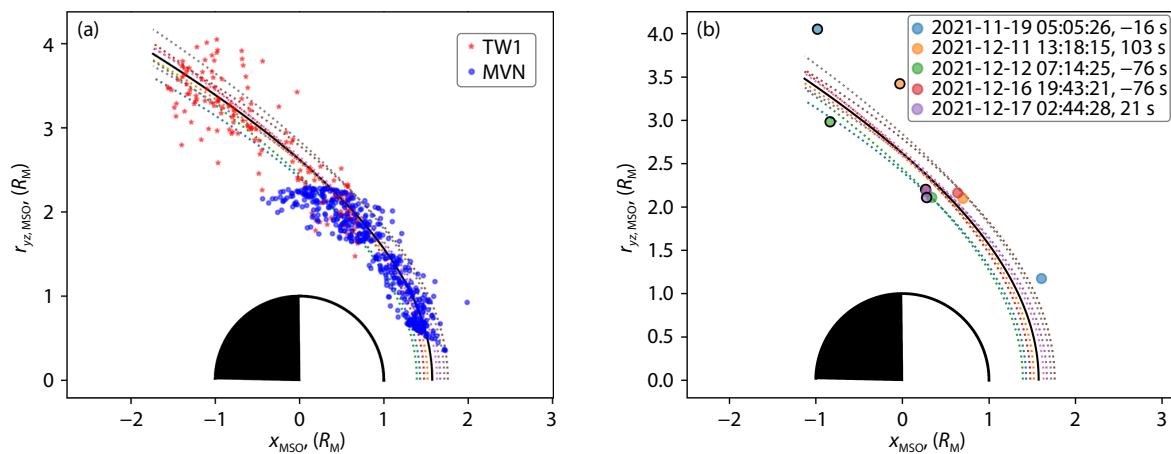


Figure 4. The bow shock (BS) crossings during the period of interest. In Panel (a), the red asterisks indicate the BS crossings of Tianwen-1's orbiter, and the blue dots the BS crossings of MAVEN. The modeled average BS (Edberg et al., 2008) is displayed by the black line; the dashed lines display the BS when uncertainties of the BS model parameters are considered. Panel (b) shows the 5 pairs of simultaneous (within 2 minutes) BS crossings of the Tianwen-1's orbiter and MAVEN. Each pair is indicated with the dots of the same color, but the dots of Tianwen-1 are enclosed by black circles. The BS crossing time of the Tianwen-1's orbiter is given in the upper-right corner followed by a time interval, with positive values meaning the later BS crossing of MAVEN. All these data are presented in the aberrated MSO coordinates.

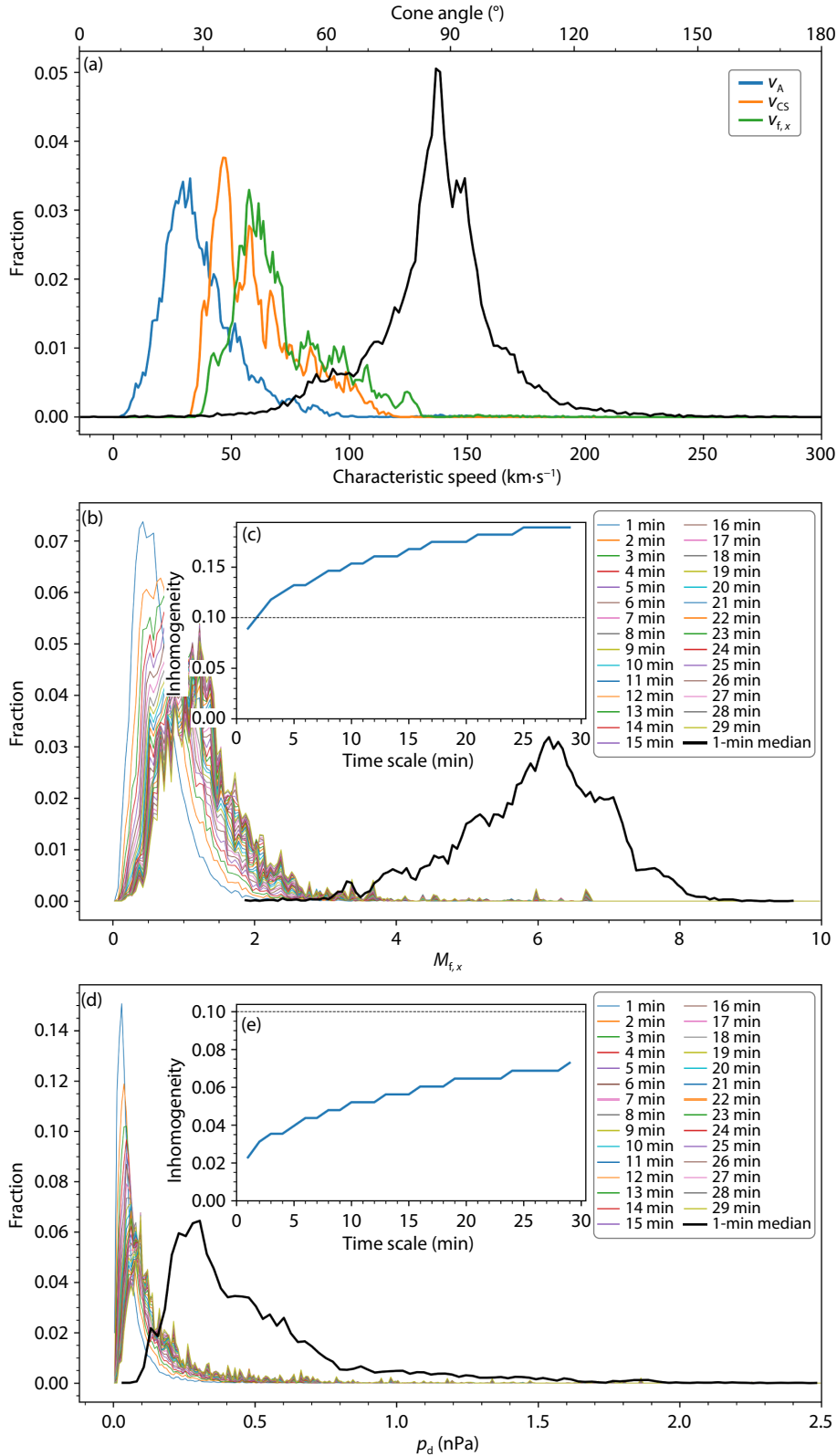


Figure 5. Characteristic speeds and inhomogeneities of solar wind fast Mach number and dynamic pressure based on MAVEN data. Panel (a) shows the distributions of the one-minute-averaged Alfvén speed (blue), sound speed (orange), and the fast-mode magnetoacoustic speed along the x direction in MSO coordinates (green) from November 13 to December 31, 2021. The black line gives the distribution of the absolute value of the angle between the minute-by-minute-averaged magnetic field vector and the x direction. Panel (b) shows the distributions of the range of the fast-mode Mach number along the x direction, $M_{f,x}$ within the various time scales, and the distribution of the one-minute-averaged $M_{f,x}$ (see the main text for details). Panel (c) gives the inhomogeneity as a function of time scale. The definition of inhomogeneity here can be found in the main text. Panels (d) and (e) are for solar dynamic pressure, with the same arrangement as Panels (b) and (c).

as shown in Figure 5d and e. The dynamic pressure also shows a single-peak distribution ranging from about 0.01 nPa to nearly 2.5 nPa with mode around 0.3 nPa. The inhomogeneity of p_d also increases as the time scale increases. By setting the dynamic range of p_d to be 2, we find that the inhomogeneity is less than 0.1 even at the time scale of 30 minutes. This suggests that M_{fx} is much more dynamic than p_d in the upstream of the Martian BS.

Based on the above analysis, we search for pairs of BS-crossing by Tianwen-1 and MAVEN that occur within 2 minutes of each other; a total of five pairs are found. We plot the paired results in Figure 4b. A first impression is that the global shape of the BS is slightly more flattened than the model. But this just reflects the south-north asymmetry of the Martian BS (e.g., Edberg et al., 2008;

Dubin et al., 2008); the Tianwen-1 orbiter crossed the southern flank of the BS, while MAVEN crossed the BS at low latitude on the northern hemisphere.

Figures 6–10 show the 5 pairs of the BS crossings. Around 05:05 UT on November 19, when the Tianwen-1 orbiter was far above the southern pole of Mars and MAVEN was close to the BS nose (see Figure 6), both spacecraft crossed the BS from the solar wind into the magnetosheath. The magnetic fields in the solar wind, measured before they entered the magnetosheath, look quite similar. Between 04:56 and 05:00 UT, we can see large variation patterns in the three components of the magnetic fields without a significant change in the total magnitude, which are probably features of an Alfvén wave. This featured structure arrived later at

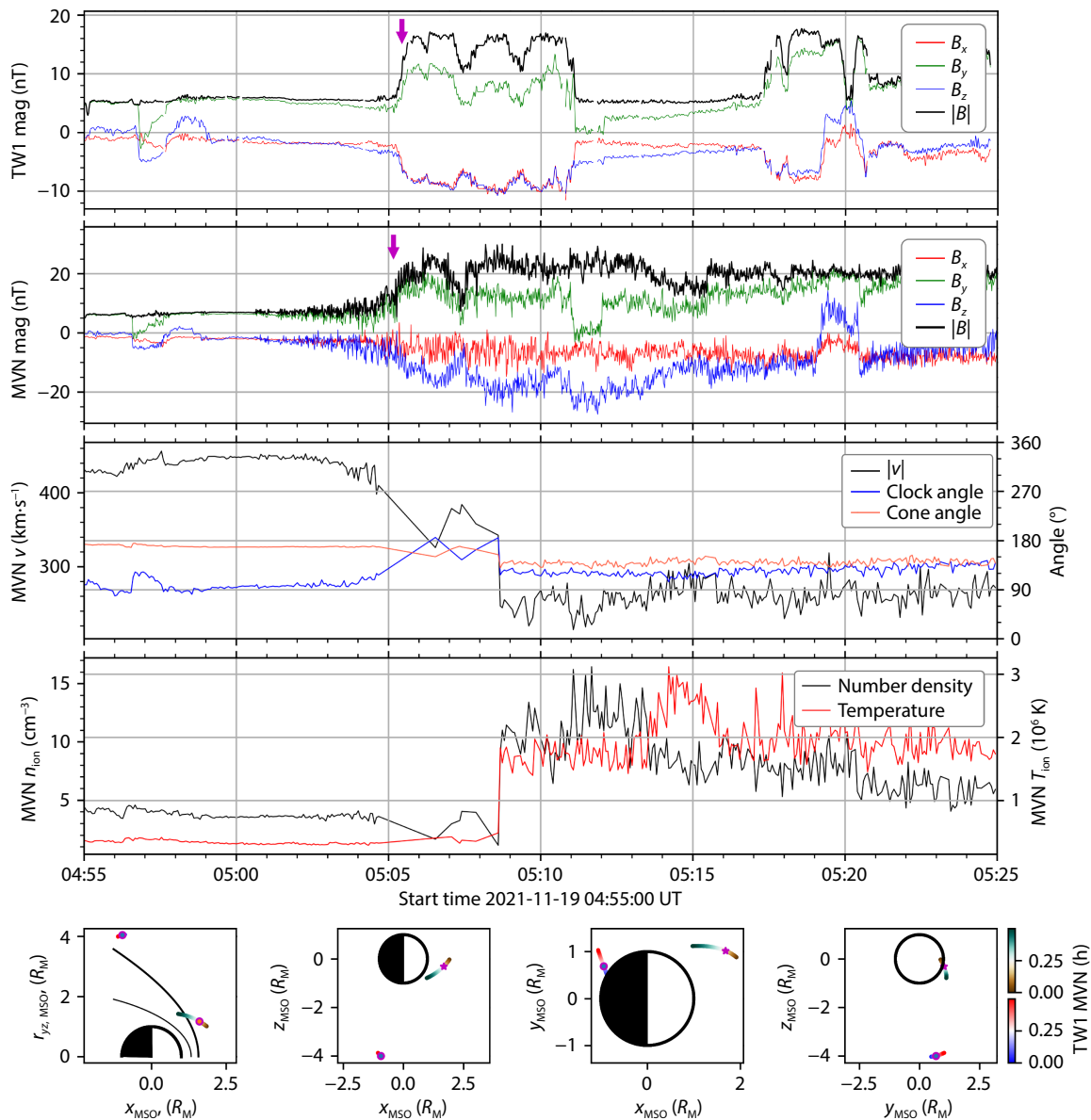


Figure 6. The simultaneous bow shock crossing around 05:05 UT on November 19, 2021. From the top to bottom, the panels display the magnetic field measured by MOMAG, the magnetic field measured by MAVEN/MAG, and the solar wind velocity, the number density and temperature of ions measured by MAVEN/SWIA, and the orbits of Tianwen-1's orbiter and MAVEN viewed from different angles. The purple arrows in the first two panels indicate the times of the bow shock crossings, and the markers in the panels on the bottom indicate the positions of the crossings.

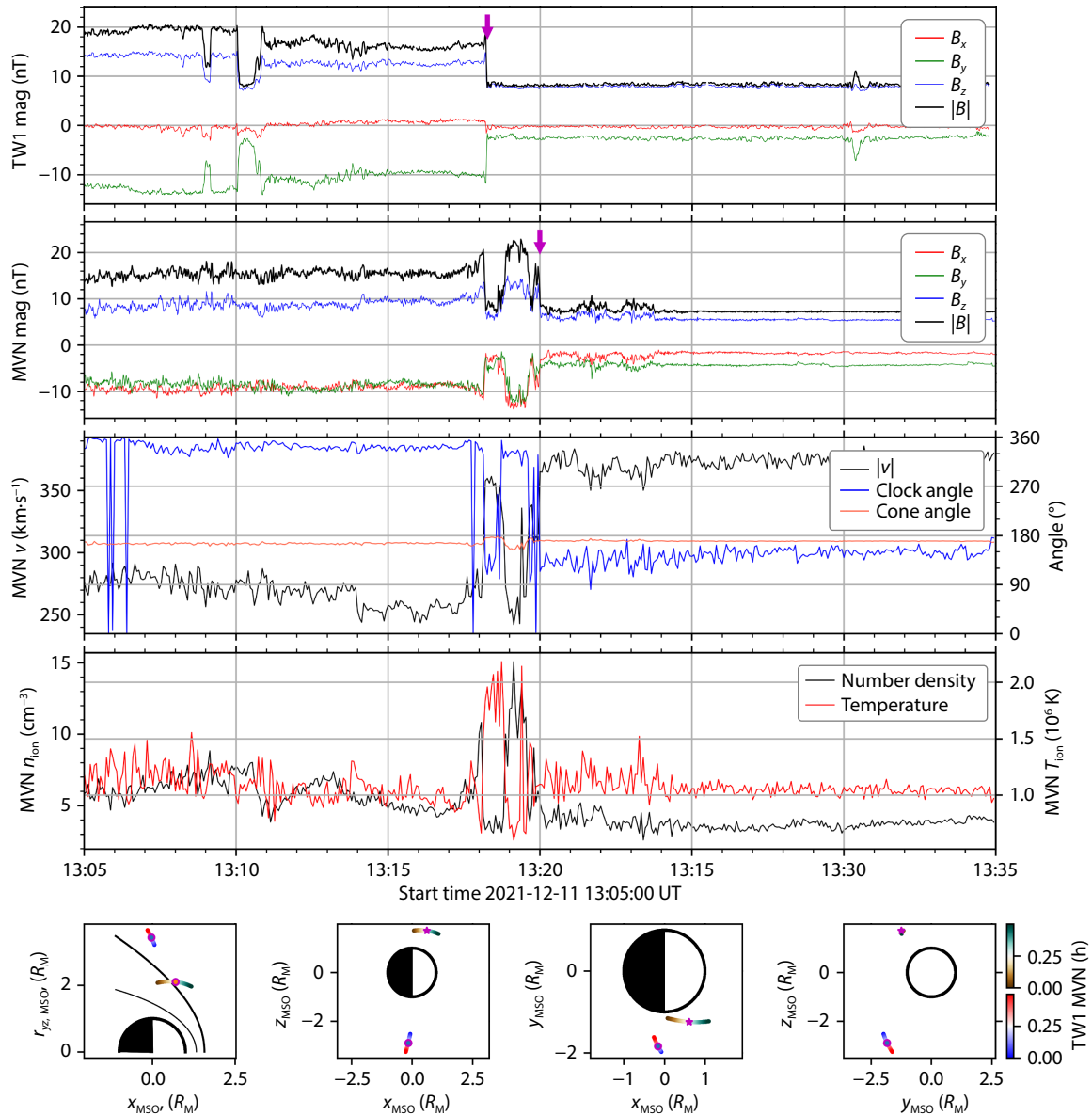


Figure 7. The simultaneous bow shock crossing around 13:19 UT on December 11, 2021.

the Tianwen-1 orbiter by about 16 s than at MAVEN, which was roughly the time spent by the solar wind travelling from MAVEN to Tianwen-1.

The magnetic fields measured by the two spacecraft after they crossed the BS show different patterns. From the first panel of Figure 6, it appears that the Tianwen-1 orbiter crossed the BS six times within 7 minutes, finally returning back to the solar wind at 05:11:10 UT, and, at about 05:17:20 UT, starting to cross the BS again. Unlike Tianwen-1, MAVEN stayed in the magnetosheath after the crossing except for turning back once at around 05:07:30 UT. This case is similar to the case shown in Figures 2h and 3h, in which the Tianwen-1 orbiter crossed the BS three times in 7 minutes but MAVEN had only one clear crossing. These phenomena suggest that the Martian BS is very dynamic at a time scale even less than one minute, and that the BS flank is more dynamic than the nose during this time period. Such multiple-crossings in minutes deserve further study, especially for events in which the Tianwen-1 orbiter crosses the BS while MAVEN remains in the

solar wind monitoring the upstream condition.

The second pair of the BS crossings is found around 13:19 UT on December 11 as shown in Figure 7. Both spacecraft were crossing the BS from the magnetosheath to the solar wind. We can see a sharp jump at 13:18:15 UT in the MOMAG data, and a sharp jump at 13:19:58 UT in the MAVEN/MAG data. In both, we also note a large dip in the total magnetic field strength. It is hard to determine if these two features are correlated. The third pair occurred at around 07:14 UT on December 12 with one probe crossing from the solar wind into the magnetosheath and the other from magnetosheath into solar wind (Figure 8). The fourth pair was at around 19:43 UT on December 16; in this instance, both spacecraft travelled from the magnetosheath into the solar wind (Figure 9). The last pair is found around 02:45 UT on December 17. Again, both spacecraft travelled from the magnetosheath into the solar wind (Figure 10). Looking at the total strengths of the magnetic fields in the magnetosheath for all the BS crossing pairs, we note that they are more or less similar no matter how large the distance

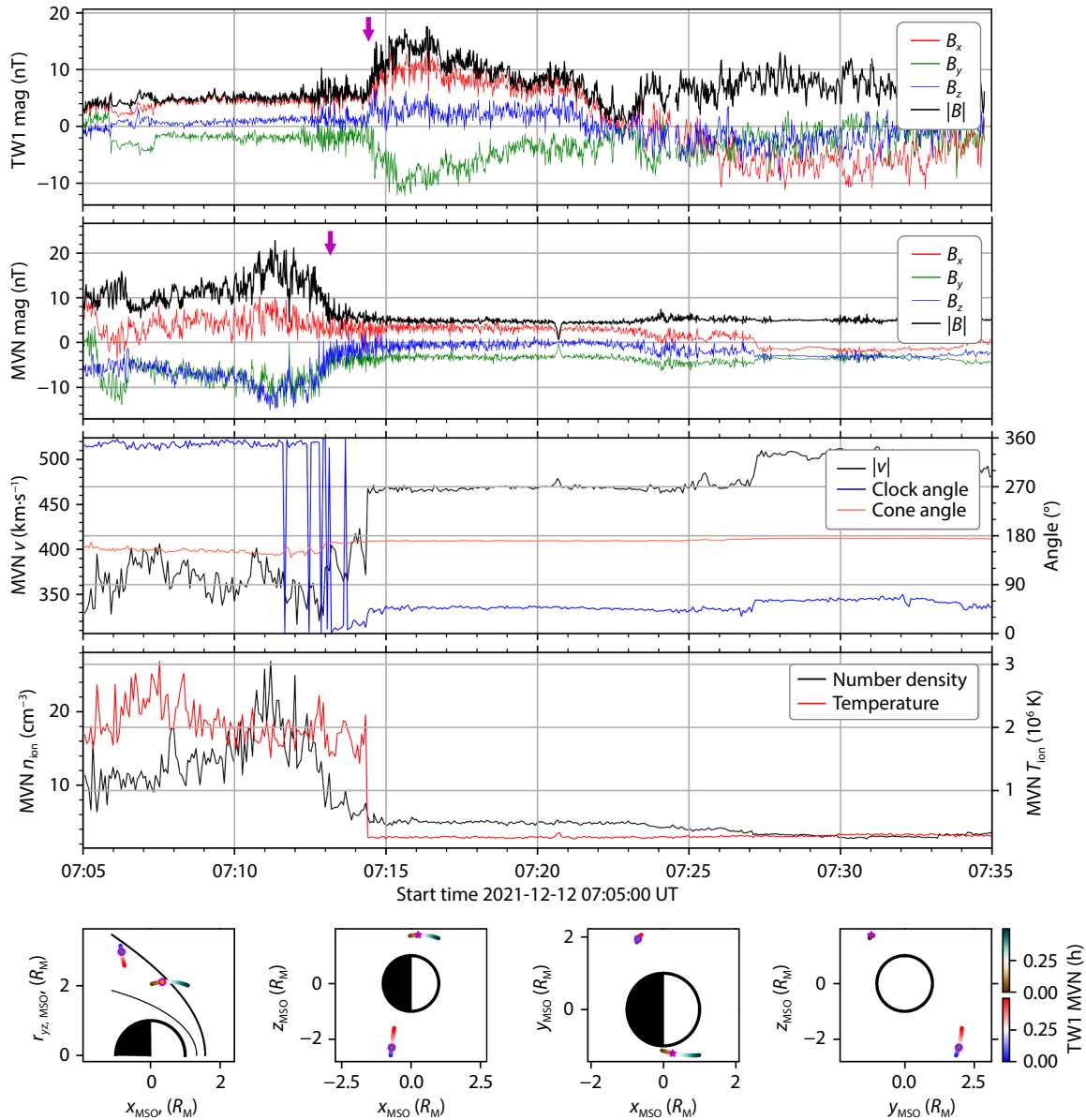


Figure 8. The simultaneous bow shock crossing around 07:14 UT on December 12, 2021.

between the two spacecraft, suggesting large-scale consistency of the global magnetic structure surrounding Mars.

4. Summary

We have presented in-flight performance of, and first results from, the Tianwen-1/MOMAG, focusing on data relevant to the most notable structure — the Martian BS. Based on the first one and a half months’ data, we identified 158 clear BS crossings, and report that their locations are statistically consistent with the BS model. Simultaneous BS crossings by Tianwen-1 and MAVEN appear to verify the south-north asymmetry of the Martian BS. The first pair of simultaneous BS crossings, along with the BS crossing case on December 30, suggest that the BS is probably more dynamic at flank than near the nose. By comparing Tianwen-1 MOMAG with MAVEN observations, we also found similar structures propagating with the solar wind from MAVEN to the Tianwen-1 orbiter. We conclude that MOMAG’s performance is excellent, providing accu-

rate measurements of magnetic field vectors. MOMAG has scanned the magnetic field in the MPR, magnetosheath, and solar wind near the dawn-dusk side. These measurements supplement MAVEN data and promise to increase significantly our understanding of the plasma environment surrounding Mars.

Acknowledgments

We acknowledge the use of data from the MAG and SWIA onboard MAVEN spacecraft, which we obtained from the NASA Planetary Data System (<https://pds-ppi.igpp.ucla.edu/>). One may apply for the Tianwen-1/MOMAG data at CNSA Data Release System (<http://202.106.152.98:8081/marsdata/>) or can download the data used in this paper from the official website of the MOMAG team (http://space.ustc.edu.cn/dreams/tw1_momag/). This work is supported by the NSFC (Grant Nos 42130204 and 42188101) and the Strategic Priority Program of the Chinese Academy of Sciences (Grant No. XDB41000000). Y.W. is particularly

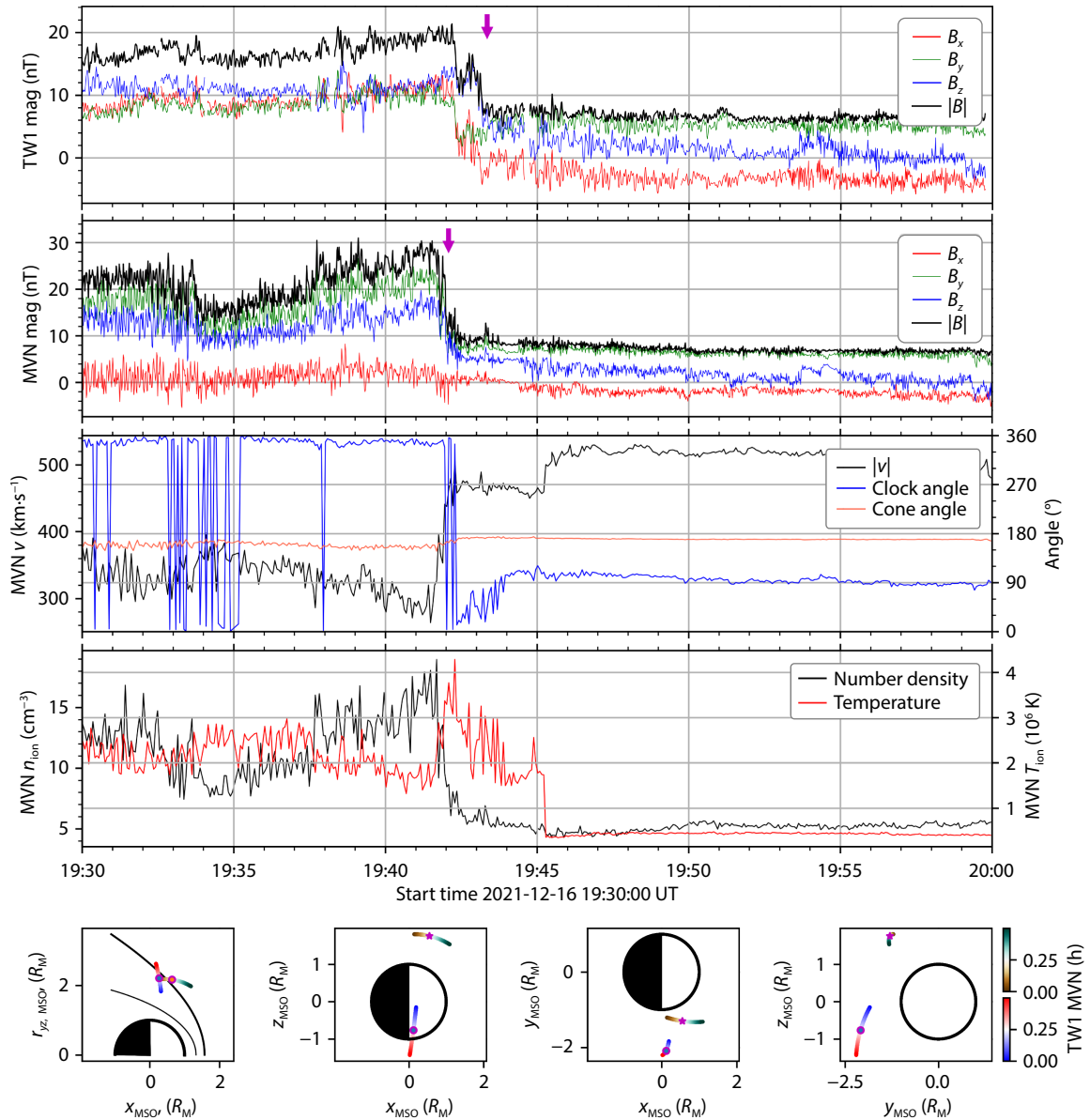


Figure 9. The simultaneous bow shock crossing around 19:43 UT on December 16, 2021.

grateful for the support of the Tencent Foundation.

References

Bertucci, C., Mazelle, C., Crider, D. H., Mitchell, D. L., Sauer, K., Acuña, M. H., Connerney, J. E. P., Lin, R. P., Ness, N. F., and Winterhalter, D. (2004). MGS MAG/ER observations at the magnetic pileup boundary of Mars: Draping enhancement and low frequency waves. *Adv. Space Res.*, 33(11), 1938–1944. <https://doi.org/10.1016/j.asr.2003.04.054>

Brain, D. A., Halekas, J. S., Peticolas, L. M., Lin, R. P., Luhmann, J. G., Mitchell, D. L., Delory, G. T., Bougher, S. W., Acuña, M. H., and Rème, H. (2006). On the origin of aurorae on Mars. *Geophys. Res. Lett.*, 33(1), L01201. <https://doi.org/10.1029/2005GL024782>

Brain, D. A., McFadden, J. P., Halekas, J. S., Connerney, J. E. P., Bougher, S. W., Curry, S., Dong, C. F., Dong, Y., Eparvier, F., ... Seki, K. (2015). The spatial distribution of planetary ion fluxes near Mars observed by MAVEN. *Geophys. Res. Lett.*, 42(21), 9142–9148. <https://doi.org/10.1002/2015GL065293>

Connerney, J. E. P., Espley, J., Lawton, P., Murphy, S., Odom, J., Oliverson, R., and Sheppard, D. (2015). The MAVEN magnetic field investigation. *Space Sci. Rev.*, 195(1), 257–291. <https://doi.org/10.1007/s11214-015-0169-4>

Dubinin, E., Modolo, R., Fraenz, M., Woch, J., Duru, F., Akalin, F., Gurnett, D., Lundin, R., Barabash, S., ... Picardi, G. (2008). Structure and dynamics of the solar wind/ionosphere interface on Mars: MEX-ASPERA-3 and MEX-MARSIS observations. *Geophys. Res. Lett.*, 35(11), L11103. <https://doi.org/10.1029/2008GL033730>

Edberg, N. J. T., Lester, M., Cowley, S. W. H., and Eriksson, A. I. (2008). Statistical analysis of the location of the Martian magnetic pileup boundary and bow shock and the influence of crustal magnetic fields. *J. Geophys. Res.: Space Phys.*, 113(A8), A08206. <https://doi.org/10.1029/2008JA013096>

Ergun, R. E., Andersson, L., Peterson, W. K., Brain, D., Delory, G. T., Mitchell, D. L., Lin, R. P., and Yau, A. W. (2006). Role of plasma waves in Mars’ atmospheric loss. *Geophys. Res. Lett.*, 33(14), L14103. <https://doi.org/10.1029/2006GL025785>

Halekas, J. S., Ruhunusiri, S., Harada, Y., Collinson, G., Mitchell, D. L., Mazelle, C., McFadden, J. P., Connerney, J. E. P., Espley, J. R., ... Jakosky, B. M. (2017). Structure, dynamics, and seasonal variability of the Mars-solar wind interaction: MAVEN solar wind ion analyzer in-flight performance and science results. *J. Geophys. Res.: Space Phys.*, 122(1), 547–578. <https://doi.org/10.1002/2016JA023167>

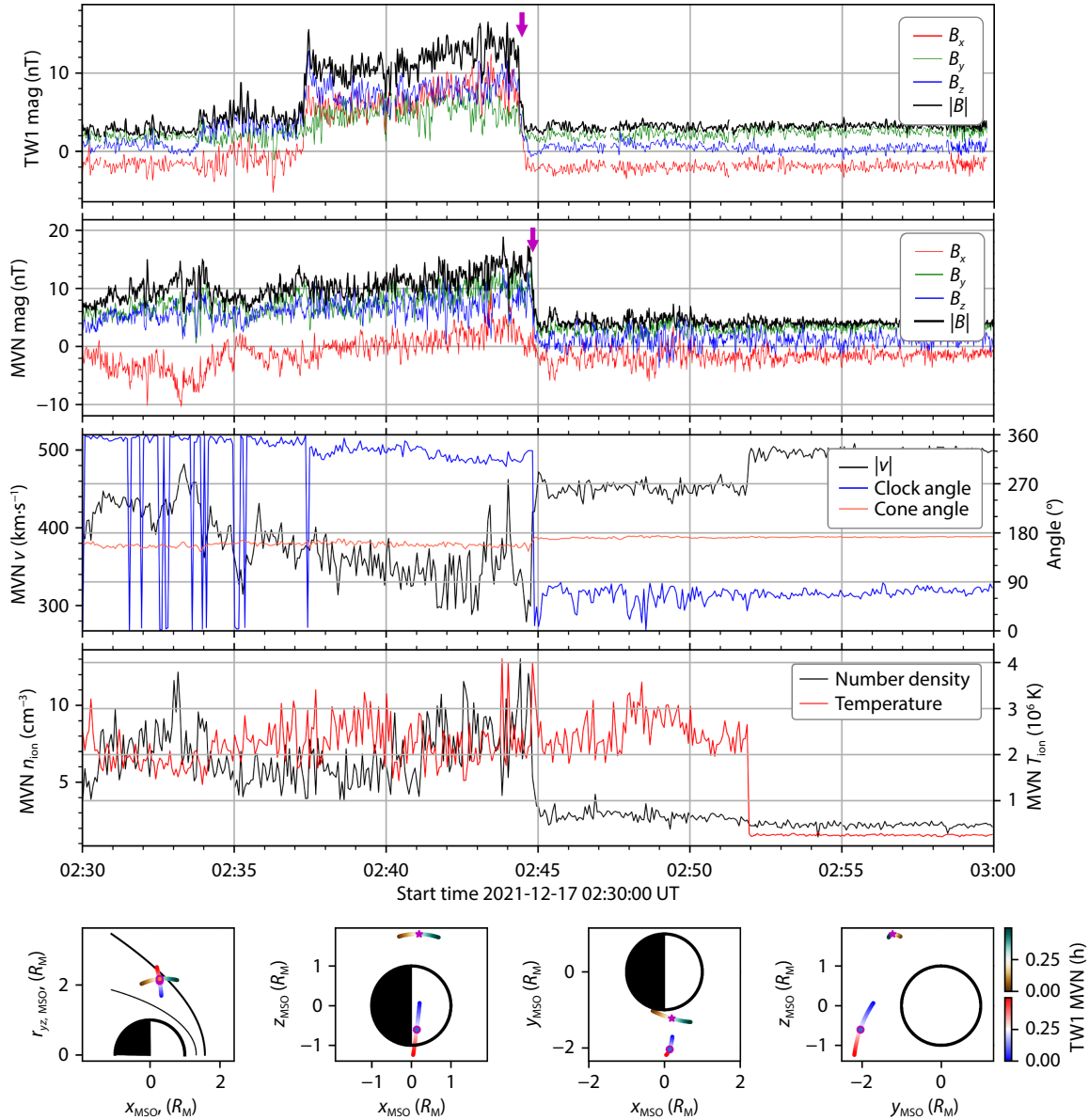


Figure 10. The simultaneous bow shock crossing around 02:44 UT on December 17, 2021.

Hall, B. E. S., Sánchez-Cano, B., Wild, J. A., Lester, M., and Holmström, M. (2019). The Martian bow shock over solar cycle 23-24 as observed by the Mars express mission. *J. Geophys. Res.: Space Phys.*, 124(6), 4761–4772. <https://doi.org/10.1029/2018JA026404>

Jakosky, B. M., Lin, R. P., Grebowsky, J. M., Luhmann, J. G., Mitchell, D. F., Beutelschies, G., Priser, T., Acuna, M., Andersson, L., ... Zurek, R. (2015a). The Mars Atmosphere and Volatile Evolution (MAVEN) mission. *Space Sci. Rev.*, 195(1), 3–48. <https://doi.org/10.1007/s11214-015-0139-x>

Jakosky, B. M., Grebowsky, J. M., Luhmann, J. G., Connerney, J., Eparvier, F., Ergun, R., Halekas, J., Larson, D., Mahaffy, P., ... Yelle, R. (2015b). MAVEN observations of the response of Mars to an interplanetary coronal mass ejection. *Science*, 350(6261), aad0210. <https://doi.org/10.1126/science.aad0210>

Liu, K., Hao, X. J., Li, Y. R., Zhang, T. L., Pan, Z. H., Chen, M. M., Hu, X. W., Li, X., Shen, C. L., and Wang, Y. M. (2020). Mars orbiter magnetometer of China's first Mars mission Tianwen-1. *Earth Planet. Phys.*, 4(4), 384–389. <https://doi.org/10.26464/epp2020058>

Mazelle, C., Winterhalter, D., Sauer, K., Trotignon, J. G., Acuña, M. H., Baumgärtel, K., Bertucci, C., Brain, D. A., Brecht, S. H., ... Slavin, J. (2004). Bow shock and

upstream phenomena at Mars. *Space Sci. Rev.*, 111(1), 115–181. <https://doi.org/10.1023/B:SPAC.0000032717.98679.d0>

Pope, S. A., Zhang, T. L., Balikhin, M. A., Delva, M., Hvizdos, L., Kudela, K., and Dimmock, A. P. (2011). Exploring planetary magnetic environments using magnetically unclean spacecraft: A systems approach to VEX MAG data analysis. *Ann. Geophys.*, 29(4), 639–647. <https://doi.org/10.5194/angeo-29-639-2011>

Ramstad, R., Barabash, S., Futaana, Y., and Holmström, M. (2017). Solar wind- and EUV-dependent models for the shapes of the Martian plasma boundaries based on Mars Express measurements. *J. Geophys. Res.: Space Phys.*, 122(7), 7279–7290. <https://doi.org/10.1002/2017JA024098>

Ruhunusiri, S., Halekas, J. S., Espley, J. R., Mazelle, C., Brain, D., Harada, Y., Dibaccio, G. A., Livi, R., Larson, D. E., ... Howes, G. G. (2017). Characterization of turbulence in the Mars plasma environment with MAVEN observations. *J. Geophys. Res.: Space Phys.*, 122(1), 656–674. <https://doi.org/10.1002/2016JA023456>

Russell, C. T., and Blanco-Cano, X. (2007). Ion-cyclotron wave generation by planetary ion pickup. *J. Atmos. Sol.-Terr. Phys.*, 69(14), 1723–1738. <https://doi.org/10.1016/j.jastp.2007.02.014>

- Wan, W. X., Wang, C., Li, C. L., and Wei, Y. (2020). China's first mission to Mars. *Nat. Astron.*, 4(7), 721–721. <https://doi.org/10.1038/s41550-020-1148-6>
- Wang, G. Q., and Pan, Z. H. (2021). A new method to calculate the fluxgate magnetometer offset in the interplanetary magnetic field: 1. Using Alfvén Waves. *J. Geophys. Res.: Space Phys.*, 126(4), e2020JA028893. <https://doi.org/10.1029/2020JA028893>
- Zhang, T. L., Delva, M., Baumjohann, W., Volwerk, M., Russell, C. T., Barabash, S., Balikhin, M., Pope, S., Glassmeier, K. H., ... Zambelli, W. (2008). Initial Venus express magnetic field observations of the Venus bow shock location at solar minimum. *Planet. Space Sci.*, 56(6), 785–789. <https://doi.org/10.1016/j.pss.2007.09.012>
- Zhang, T. L., Lu, Q. M., Baumjohann, W., Russell, C. T., Fedorov, A., Barabash, S., Coates, A. J., Du, A. M., Cao, J. B., ... Balikhin, M. (2012). Magnetic reconnection in the near Venusian magnetotail. *Science*, 336(6081), 567–570. <https://doi.org/10.1126/science.1217013>
- Zou, Y. L., Zhu, Y., Bai, Y. F., Wang, L. G., Jia, Y. Z., Shen, W. H., Fan, Y., Liu, Y., Wang, C., ... Peng, Y. Q. (2021). Scientific objectives and payloads of Tianwen-1, China's first Mars exploration mission. *Adv. Space Res.*, 67(2), 812–823. <https://doi.org/10.1016/j.asr.2020.11.005>
- Zou, Z. X., Wang, Y. M., Zhang, T. L., Wang, G. Q., Xiao, S. D., Pan, Z. H., Zhang, Z. B., Yan, W., Du, Y., ... Guo, J. N. (2023). In-flight calibration of the magnetometer on the mars orbiter of Tianwen-1. *Sci. China Tech. Sci.*, submitted. <https://arxiv.org/abs/2302.04671>